

Recent advances to accelerate re-endothelialization for vascular stents

Journal of Tissue Engineering
Volume 8: 1–14
© The Author(s) 2017
Reprints and permissions:
sagepub.co.uk/journalsPermissions.nav
DOI: 10.1177/2041731417731546
journals.sagepub.com/home/tej



Tarek M Bedair^{1,2}, Mahmoud A EINaggar^{1,3},
Yoon Ki Joung^{1,3} and Dong Keun Han^{1,3,4}

Abstract

Cardiovascular diseases are considered as one of the serious diseases that leads to the death of millions of people all over the world. Stent implantation has been approved as an easy and promising way to treat cardiovascular diseases. However, in-stent restenosis and thrombosis remain serious problems after stent implantation. It was demonstrated in a large body of previously published literature that endothelium impairment represents a major factor for restenosis. This discovery became the driving force for many studies trying to achieve an optimized methodology for accelerated re-endothelialization to prevent restenosis. Thus, in this review, we summarize the different methodologies opted to achieve re-endothelialization, such as, but not limited to, manipulation of surface chemistry and surface topography.

Keywords

Stent, restenosis, biomolecules, surface modification, re-endothelialization

Date received: 30 April 2017; accepted: 19 August 2017

Introduction

The heart is supplied with oxygenated blood through what is called the coronary artery. The narrowing of these arteries due to plaque decreases the oxygen supply to the cardiac muscles leading to the most common type of heart disease, and the most common cause of death since 2012, called coronary artery disease.^{1,2} This drove the researcher for decades to find a treatment for this disease.

In 1980, Gruentzig and colleagues reported for the first time a method for revascularization of occluded coronary arteries, called percutaneous coronary intervention or as it is widely known as ballooning.³ The procedure was done by inserting a balloon catheter into the arteries until it reaches the lesion site; by the aid of water pressure, the balloon expands thus unblocking the artery.⁴ Despite the success of this procedure, the high rate of restenosis (30%–50%) remained an issue that needed a solution.⁵

Since the development of the balloon angioplasty, new candidates were fabricated to try and overcome the shortcomings. The development of bare metal stents (BMSs) followed by drug-eluting stents (DESs) revolutionized angioplasty in recent years, with many new candidates hitting the market. The basic idea of the metallic stent is to provide mechanical support to the vascular walls and

prevent the recoil of artery at the lesion site. However, the drugs that coat the surface are to prevent inflammation and the proliferation of smooth muscle cells (SMCs) due to vascular wall injury caused by the deployment of the stent.¹ Several studies to optimize the coating conditions⁶ and to improve the stability of the drug-in-polymer matrix coating were developed for further enhancing the efficacy

¹Center for Biomaterials, Korea Institute of Science and Technology (KIST), Seoul, Korea

²Chemistry Department, Faculty of Science, Minia University, Minia, Egypt

³Department of Biomedical Engineering, Korea University of Science and Technology, Daejeon, Korea

⁴Department of Biomedical Science, CHA University, Gyeonggi, Korea

Corresponding authors:

Dong Keun Han, Center for Biomaterials, Korea Institute of Science and Technology (KIST), 5, Hwarang-ro 14-gil, Seongbuk-gu, Seoul 02792, Korea.

Email: dkh@kist.re.kr; dkhan@cha.ac.kr

Yoon Ki Joung, Center for Biomaterials, Korea Institute of Science and Technology (KIST), 5, Hwarang-ro 14-gil, Seongbuk-gu, Seoul 02792, Korea.

Email: ykjoung@kist.re.kr



Creative Commons Non Commercial CC BY-NC: This article is distributed under the terms of the Creative Commons

Attribution-NonCommercial 4.0 License (<http://www.creativecommons.org/licenses/by-nc/4.0/>) which permits non-commercial use, reproduction and distribution of the work without further permission provided the original work is attributed as specified on the SAGE and Open Access page (<https://us.sagepub.com/en-us/nam/open-access-at-sage>).

of DESs under *in vitro* as well as *in vivo* clinical studies.^{7–11}

However, despite their infamous reputation and their ability to suppress restenosis to large extent, they still led to important side effects such as late thrombosis, delayed re-endothelialization, medial necrosis, and chronic inflammation.^{12–15}

It has been unveiled by a copious body of studies that late stent thrombosis is caused by the impaired endothelial cells (ECs) growth on the luminal side of the artery.^{16–19} Thus, attempts to fabricate new platforms that will encourage the proliferation of ECs would be a huge step forward in the field of biomedical devices. The optimal implant surface is that surface which could (a) prevent the adsorption of fibrinogen; (b) prevent the adhesion, aggregation, and activation of platelet; (c) inhibit the adhesion and proliferation of SMCs; and (d) promote the adhesion and growth of ECs (Figure 1).

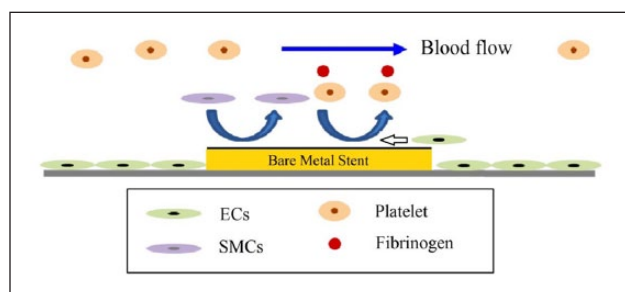


Figure 1. Schematic representation of the optimal surface for stent application.

ECs: endothelial cells; SMCs: smooth muscle cells.

In this review, we summarized for the reader the recent studies that have attempted various approaches to achieve such a platform, beginning with studies that have researched the effects of manipulating the surface chemistry of different platforms on ECs proliferation and ending with the studies that researched the physical tuning of these surfaces.

Biomolecules for re-endothelialization

Several molecules have been used to improve the cell-material interactions in order to enhance the adhesion and growth of ECs and consequently accelerate re-endothelialization, for example, heparin, fucoidan, chondroitin sulfate, hyaluronic acid, antioxidant compounds, and extracellular matrix (ECM) proteins including laminin, fibronectin, and collagen (I). The chemical structures of these molecules are summarized in Figure 2.

Heparin is a highly sulfated glycosaminoglycan which consists of uronic acid and glucosamine, commonly used as anticoagulant drug to prevent thrombosis on metal stents²⁰ and anti-inflammatory drug for treatment of chronic obstructive bronchopulmonary disease.²¹ The mechanism of anticoagulant action of heparin occurs through the reaction with antithrombin III, which inactivates the thrombin and other proteases involved in the blood clot.^{22,23} Several studies have shown that heparin-modified substrates could prevent platelet adhesion and inhibit the growth and suppress the proliferation of SMCs.²⁴ In 2016, Pan et al.²⁵ have proposed a new strategy to improve both of blood and endothelial cells compatibility by modifying the titanium substrate with polydopamine followed by the deposition of graphene oxide and finally loaded with heparin. *In vivo* animal study

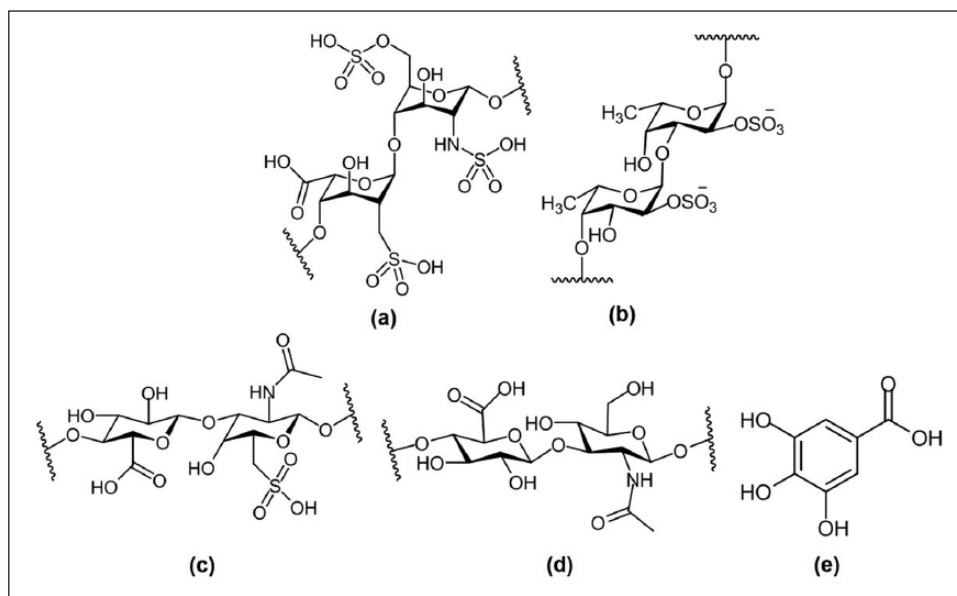


Figure 2. The chemical structure of biomolecules used to promote the growth of endothelial cells: (a) heparin, (b) fucoidan, (c) chondroitin sulfate, (d) hyaluronic acid, and (e) gallic acid.

proved that heparin-coated stent prevents thrombosis and in-stent restenosis.²⁶

Fucoidan is a sulfated polysaccharide extracted from brown seaweed with anticoagulant efficiency similar to heparin. It has various pharmacological activities such as anti-thrombosis, anti-viral, anti-cancer, anti-angiogenic, and anti-inflammatory effects.^{27–31} It has been demonstrated that low-molecular-weight fucoidan (LMWF) reduces the proliferation of SMCs and consequently prevents neointimal hyperplasia in rabbit model.^{32–34} Roux et al.³⁵ showed an early endothelial repair for an aortic allograft model. LMWF significantly reduced intimal hyperplasia after 21 days which was associated with intimal re-endothelialization due to recruitment of bone-marrow-derived, properly, endothelial progenitor cells (EPCs).³⁵ The mechanism of action of LMWF on cell signaling and whole genome expression in ECs was recently studied.³⁶ They found that LMWF was able to trigger the activation of PI3K/AKT pathways which plays an important role in angiogenesis and vasculogenesis. Moreover, LMWF modulated the expression of genes involved in cell migration and cytoskeleton organization, cell mobilization, and homing.³⁶

Chondroitin sulfate, is a sulfated polysaccharide composed of glucuronic acid and galactosamine, which have the ability to enhance the resistance of vascular cell apoptosis.³⁷ In addition, sulfated polysaccharides can improve the hemocompatibility of implant surface through electrostatic repulsion toward negatively charged blood components such as fibrinogen.³⁸

Hyaluronic acid is a negatively charged non-sulfated polysaccharide composed of *N*-acetyl glucosamine and *D*-glucuronic acid which is a component of ECM.^{39–42} It was demonstrated that hyaluronic acid plays a role in cell attachment and signaling through interacting with cell surface receptors. In addition, it can reduce the adhesion and aggregation of platelets when hyaluronic acid was coated on stainless steel stent.⁴³ Moreover, it displayed antifouling properties with respect to protein adsorption and marine adhesion.^{44–47}

Gallic acid is a natural plant phenol molecule derived from green teas and red wine and highly rich in beverages.^{48,49} It also has various biological activities such as anticarcinogen,^{50,51} antibacterial,⁵² antiviral,⁵³ anti-inflammatory,⁵⁴ and antitumor effects.^{55,56} In addition, it possesses arterioprotective properties due to its powerful antioxidant property. Moreover, it was found that gallic acid has no cytotoxicity against ECs, whereas it can induce SMCs death.⁵⁷ Furthermore, the loading amount of gallic acid could govern the behavior of vascular cells on the stent surface. It was demonstrated that 5 $\mu\text{g}/\text{mL}$ can selectively promote ECs growth and inhibit SMCs proliferation.⁵⁸

Laminins are family of glycoproteins located in basement membranes and play an important role to mediate both cell-to-cell and cell-to-extracellular matrix adhesion and to enhance cell differentiation and proliferation.⁵⁹

Fibronectin is a major component found in ECM consisting of two monomers linked by a disulfide bond at their C-termini.⁶⁰ It has the ability to be adsorbed or conjugated with biomaterial surfaces to promote the attachment, spreading, and differentiation of ECs.^{61,62} Arginine-glycine-asparagine (RGD) domains in the fibronectin molecule was considered as a key motif interaction with $\alpha 5\beta 1$ transmembrane integrin receptor of cells.^{63,64}

Ways to improve re-endothelialization

According to the recent reports for accelerating re-endothelialization, three possible ways were used including changing the chemistry of the implant surface, changing the surface topography of the implant, and changing both of topography and chemistry of the implant surfaces. These ways will be discussed in detail in the following sections.

Surface chemistry on re-endothelialization

The chemistry of the surface plays a crucial role to decide the hemocompatibility and cytocompatibility with blood components and arterial cells, respectively. There are several methods to change the chemistry of the surface through direct immobilization, layer-by-layer (LBL) techniques, or nitric oxide (NO) release system. Moreover, methods and recent findings regarding antibody immobilization on material surfaces have been summarized elsewhere.^{65,66}

Direct immobilization on metal surface. In the recent years, immobilizing biomolecules on biomaterials surface has attracted great attention by researchers. However, the stability of these molecules under *in vivo* exposure remains a question for successful clinical treatment. Many methods could be achieved to immobilize biomolecules on implant surface such as physical adsorption, encapsulation, ionic bonding, and covalent bond formation. Covalent immobilization in which the molecules will be stable on the surface and not easy to remove by rising to withstand under *in vivo* exposure was considered as the most famous method. It can be performed through various chemical reactions such as Schiff base and carbodiimide chemistry. The immobilization could be performed for single or a mixture of biomolecules.

Single-molecule immobilization. In 2014, Yang et al. successfully modified the stainless steel stent using 900 ng of heparin via dip coating method. The substrate was initially coated with dopamine and hexamethylenediamine to introduce coating rich with a primary amine functional group. Then, heparin was immobilized through carbodiimide chemistry. It was found that the heparin-modified substrate

reduces the fibrinogen adsorption and platelet adhesion. In addition to selectively enhancing ECs adhesion, proliferation, migration, and NO release, SMCs adhesion and proliferation were inhibited.⁶⁷ Another group fabricated a multifunctional polymer consisting of dopamine-*g*-heparin or dopamine-*g*-heparin-like polymer (poly(sodium 4-vinylbenzenesulfonate)-*co*-poly(sodium methacrylate)) for the modification of polyethersulfone dialysis membrane.⁶⁸ The heparin-mimicking membranes presented lower protein adsorption, superior ECs proliferations and morphology differentiation, and lower platelet adhesion with excellent anticoagulant bioactivities.⁶⁸ Recently, Li et al.⁶⁹ developed heparin/poly-L-lysine microspheres and immobilized them on dopamine-coated stainless steel substrate. The microsphere formation occurred via intermolecular electrostatic interactions between positively charged poly-L-lysine and negatively charged heparin, forming spheres ranging between 300 and 1500 nm as determined by dynamic light scattering. The amine groups presented on the microspheres contributed to covalent bond formation with dopamine through Schiff base and/or Michael addition reaction. The existence of the microspheres improved the cytocompatibility, blood compatibility, and accelerate endothelialization.⁶⁹

In 2014, Thalla et al.⁷⁰ demonstrated the advantages of grafting chondroitin sulfate to glass substrate. They found that chondroitin sulfate-modified glass showed resistance to fibrinogen and platelet adhesion, which suggested that it can prevent thrombus formation. Moreover, ECs adhesion and growth were strongly promoted with complete and flow-resistant endothelium.⁷⁰

Another biomolecule, hyaluronic acid, was grafted on stent surface to achieve antifouling properties and enhance re-endothelialization. Kim et al. fabricated a DES with two different surfaces with multi-functions. First, the stent was pre-coated using dopamine-conjugated hyaluronic acid (HA-DA), followed by spray coating of sirolimus-inpoly(D,L-lactide) matrix only on the abluminal surface of stent.⁷¹ It was demonstrated that HA-DA coating displayed suppressive effects on platelet adhesion and activation and maintained the ECs viability and proliferation even under the existence of sirolimus.⁷¹ Recently, Lih et al.⁷² modified cobalt-chromium substrates with HA-DA and figure out the optimal concentration of catechol group through preparing different ratios of HA-DA ranged between 2% and 15% (50–400 μmol) in order to improve the hemocompatibility and re-endothelialization. Among these different dopamine contents, it was found that 100 μmol of dopamine demonstrated the lowest fibrinogen adsorption, the lowest platelet adhesion with no pseudopodia, and the highest ECs proliferation.⁷² Similar study to reduce the protein adsorption including fibrinogen was established by one-step process for immobilizing hyaluronic acid molecules onto gold surface via the interfacial polymerization of dopamine.⁷³

Another strategy to enhance re-endothelialization was presented in 2014 by Yang et al.⁷⁴ in which they modified the implant surface with gallic acid through two different methods: (a) carbodiimide chemistry in which the amino group of plasma-polymerized allylamine (PPAam) reacted with activated carboxyl group of gallic acid (phenolic hydroxyl groups of gallic acid were retained) and (b) Tris-buffer in which the amino group of PPAam reacted with quinone structure of gallic acid (carboxyl acid groups of gallic acid were retained). The gallic acid-functionalized surface presented selectivity toward endothelial and smooth muscle cells. It enhanced the adhesion, proliferation, migration, and release of NO of ECs. On the other hand, it inhibited the adhesion and proliferation of SMCs.⁷⁴ Interestingly, the gallic acid coating formed by Tris method presented a stronger inhibitory effect on SMCs proliferation than that formed by carbodiimide method. Similar inhibitory effect of epigallocatechin-3-*O*-gallate on SMCs was reported and attributed to the existence of galloyl group and phenolic hydroxyl group.^{75–77} Moreover, it was demonstrated that the existence of galloyl group of catechins was essential for inhibiting SMCs proliferation.^{78–80}

Multi-molecules immobilization. To achieve a microenvironment with favorable properties to enhance endothelial cell adhesion and proliferation and improve the hemocompatibility simultaneously, to ensure the long-term safety of cardiovascular implants, a mixture of biomolecules was co-immobilized on the implant surface. It is commonly known that the surface with different biomolecules may combine the properties of each individual.

In 2011, Li et al.²⁰ reported the co-immobilization of heparin and fibronectin complex on titanium substrate in order to improve the hemocompatibility and endothelialization. The coating displayed a stable behavior for 5 days in phosphate buffer, lower hemolysis, less platelet adhesion/aggregation, and lower fibrinogen adsorption. In addition, the endothelial cells presented higher adhesion and proliferation on such surface as compared to control titanium substrate.²⁰ According to He et al.,⁸¹ the polymerized acrylic acid film was modified using fibronectin through carbodiimide chemistry. The enzyme-linked immunosorbent assay results indicated the existence of RGD domains in the immobilized fibronectin on stainless steel substrate. ECs were spread well on the fibronectin-modified surface, compared to the control substrate. Further study was performed in 2014 by Wang et al.,⁸² in which the titanium substrate was functionalized with multifunctional microenvironment using heparin, fibronectin, and vascular endothelial growth factor (VEGF) (heparin/fibronectin/VEGF) to inhibit thrombosis formation and promote endothelialization. VEGF is an angiogenic growth factor that binds to VEGF receptor 1 or 2 present at the surface of endothelial cells. It has been extensively used to accelerate vascularization of damaged tissue as it plays a vital role in

orienting endothelial cells to migrate, proliferate, and form tubular structures.^{83–85} The heparin/fibronectin complex can be formed by electrostatic interaction between the negatively charged heparin and the positively charged fibronectin. In 2016, Choi et al.⁸⁶ designed a method to load VEGF and hepatocyte growth factor (HGF) on heparin-grafted HA-DA modified on cobalt-chromium substrate. They found that using divinyl sulfone method, the loading amount of heparin increased and consequently the amount of growth factor with retained bioactivity also increased. In addition, it presented higher cell viability.⁸⁶ Recently, in 2016, Ye et al. established a novel multifunctional coating consisting of fucoidan and laminin complex using carbodiimide chemistry to provide rapid endothelialization, improve hemocompatibility, and prevent restenosis.⁸⁷ This complex showed that the growth of ECs and EPCs was promoted, whereas the SMCs were inhibited. In addition, the resulting surface exhibited lower platelet adhesion with anticoagulant property.⁸⁷

Layer-by-Layer coating. LBL technique was used to build a mixture of biomolecules on the material surfaces. This method has attracted a great attention possessing many advantages such as easy preparation method, wide range of charged biomolecules can be assembled, independence on substrate shape, and mild reaction conditions.⁸⁸ It is based on the electrostatic interactions of anionic and cationic poly(electrolytes) on charged surfaces to built-up ultrathin multilayer films composed of up to 100 consecutively alternating layers.⁸⁹ An example for LBL was fucoidan/laminin-coated stent which presented good stability behavior, lower platelet adhesion, and selectively regulated vascular cells growth.^{87,90} The best hemocompatibility was achieved when fucoidan was at the outermost layer with lowest platelet adhesion when three layers of fucoidan were fabricated. On the other hand, when laminin increased to five layers, both of anticoagulant and cytocompatibility of ECs and EPCs were improved.⁹⁰ According to Wang et al.,⁹¹ the titanium surface was modified using LBL technique consisting of heparin/VEGF and terminated with fibronectin. It was suggested that fibronectin-terminated multilayer film could enhance the attachment of ECs via its RGD. VEGF could promote the adhesion and proliferation of ECs. Furthermore, the existence of heparin could reduce the platelet adhesion and aggregation. The faster proliferation of ECs and the reduction of platelet adhesion proved the concept of co-immobilization of heparin/VEGF/fibronectin.⁹¹ In 2015, Liu et al.⁹² constructed an endothelial cell extracellular microenvironment on nitinol alloy substrate via LBL assembly technique including gelatin/chitosan embedded with VEGF. It was found that this multilayer film was beneficial for ECs adhesion and proliferation. Additionally, the presented surface promoted the production of NO from the ECs.⁹²

NO release for re-endothelialization. NO is generated in healthy blood vessels by endogenous nitric oxide synthase (NOS) enzyme isoforms,⁹³ and its controlled release plays a critical role in maintaining homeostasis of blood vessels. NO has pleiotropic effects that include anti-atherogenesis, vasodilation, and inhibition of SMCs proliferation and platelet aggregation.⁹³

The dose-dependent action of NO is one of its most interesting characteristics. While picomolar and nanomolar levels of NO cause proliferation of many different cell types,⁹⁴ many reports have shown that NO donors at micromolar and millimolar levels inhibit the proliferation of certain types of cells such as SMCs,^{94–97} murine bone marrow cells,⁹⁸ and ECs.⁹⁶ A large body of literature unveiled that the lack of NO around implanted stents might cause restenosis and thrombosis, which is due to the low NO release at lesion site as the endothelial cells are injured.¹ Therefore, compensating the low level of NO is a very potential strategy for overcoming the drawbacks of stents.^{1,93,99}

Selenium catalyst NO releasing surfaces. In the human body, there are a group of compounds that release NO intrinsically called nitrosothiols, including S-nitrosoglutathione (GSNO), S-nitrosocysteine, and S-nitrosoalbumin.¹⁰⁰ Meanwhile, in vivo glutathione peroxidase (GPx) enzymes protect the cells from hydrogen peroxide by reducing it to water.¹⁰¹ During the process of reduction, glutathione is oxidized after donating an electron, not only that, but GPx also catalyzes the release of NO from the aforementioned donors in the presence of intrinsic thiols.¹⁰² Taking what was mentioned into consideration, various organoselenium compounds have been reported to have GPx-like catalytic activity, such as selenocystamine (SeCA) and selenodipropionic acid (SeDPA), thus releasing NO from nitrosothiols.^{103,104} The proposed catalytic mechanism is summarized in Scheme 1,¹⁰³ in which each species represents: diselenide (RSe-SeR), thiol (R'SH and GSH (glutathione)), selenosulfide (RSe-SR' and RSe-SG (a glutathione adduct)), selenolate (RSe⁻, a conjugate base of selenol), and S-nitrosothiol (R'SNO).

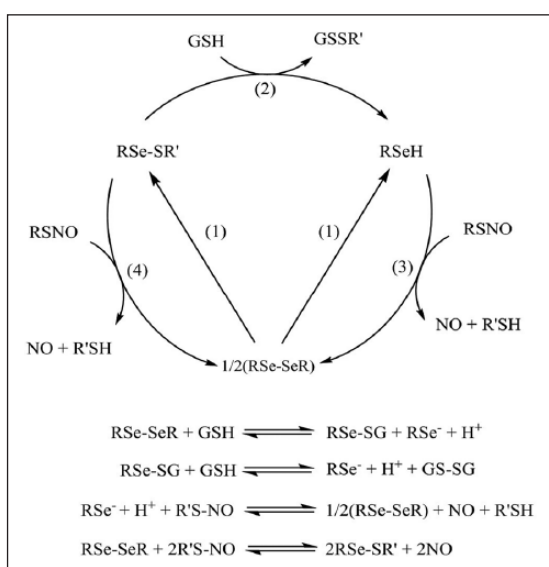
This led to various research groups to immobilize different types of selenium catalysts on surface of metallic stents in an attempt to benefit from its continuous NO release rate in regard to re-endothelialization.

In 2011, Weng et al.¹⁰⁵ fabricated NO-releasing stent with SeCA covalently immobilized on the surface, as shown in Figure 3(a). One of the limitations of fabricating such a stent is the absence of functional groups on the surface of stainless steel stents. This led the group to use titanium dioxide (TiO₂)-coated stents, which then added a layer of polydopamine thus achieving a stent with an abundant number of free hydroxyl groups. This allowed SeCA to be covalently attached to the surface via its amine group. The authors prepared two types of stents with selenium,

one with two layers of polydopamine grafted on the surface denoted as Se2 and the other one contained five layers of polydopamine denoted as Se5. Additionally, the two samples had different GPx mimicking activity, in which Se5 had significantly higher catalytic activity, but this was the case only for freshly prepared samples, as the rate decreased significantly within 3 months for both samples. In regard to the NO release rate, same as for the GPx activity, the Se5 samples had a higher NO release rate than Se2 counterpart under in vitro study using two NO donors GSNO and SNAP. Other in vitro studies were performed, such as platelet adhesion tests and SMC adhesion tests, and it was unveiled that Se5 stents outperformed the other samples, by decreasing the adhesion and activation of the

platelets and inhibiting the SMCs from attaching to the surface. After 2 months of in vivo study for femoral arteries of dogs, the stents were removed, and it was found that the stents were completely covered with shuttle-shaped endothelial cells. After analyzing cross sections of the samples, it was shown that the selenium stents have had lower intimal and neointimal thickness than that of the plain stainless steel stents.

In 2015, Yang et al.¹⁰⁶ fabricated a selenium catalyst immobilized stent with a different immobilization approach (Figure 3(b)). Instead of using a polydopamine base layer on top of the stainless steel surface, they added a layer using a methodology they standardized elsewhere,¹⁰⁷ which will provide sufficient amount of free amines on the surface for covalent attachment of SeDPA. Initially, they tested the NO catalytic activity of the surface, which showed two phases of NO release, fast release then slow release, which was according to previously published results by Cha et al. In addition, it was found out that there was 12.5% decrease in activity of the catalyst after 1 h of exposure to the NO donor, with 44% decrease after 60 days of exposure.¹⁰³ This decrease in activity could be explained by the reduction of SeDPA to selenolate by glutathione, as shown in Scheme 1. They tested the hemocompatibility and vascular cell growth behavior of the stent. The tests exhibited effective inhibition of platelet adhesion and SMCs growth and effectively enhanced ECs growth and migration when compared to the controls that include bare stainless steel and PPAam-coated stents. In vivo studies were performed by implanting the stent in rabbit iliac arteries under angiographic control for 4 weeks. The catalyst-based stents showed superior results, in which the blood clotting experiments confirmed the platelet adhesion tests. Moreover, the hematoxylin eosin-stained cross sections of the arteries demonstrated reduced neointimal hyperplasia, mean



Scheme 1. Schematic diagram for the production of NO from selenium catalyst.

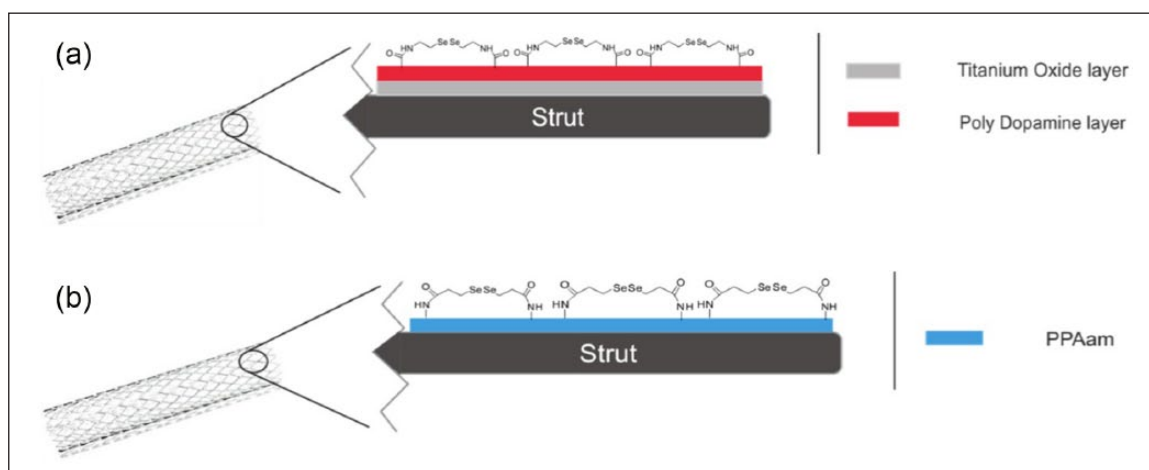


Figure 3. Schematic representation of (a) stainless steel stent covered with a layer of titanium and then another layer of polydopamine with the final surface covered with SeCA and (b) stainless steel stent covered with a layer of plasma-polymerized allylamine (PPAam) and then a final layer of SeDPA.

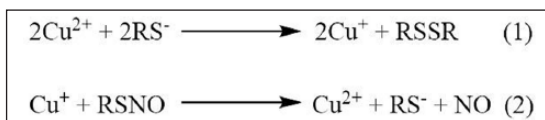
neointimal area, and neointimal stenosis. Additionally, scanning electron microscopy images indicated the stents to be fully covered with endothelial cells, whereas the bare stainless steel was not fully covered.

In another attempt, Chen et al.¹⁰⁸ took on a different approach, in which they covalently attached selenium catalyst to LBL electrospun vascular grafts on the luminal side only. First, the vascular grafts backbone was made up of polycaprolactone electrospun films. Then, a layer of polylysine was added as the base layer on the luminal side of the graft, which was then followed by a polyglutamic acid layer with a negative charge and a free carboxyl group facing outward. These free carboxyl groups would react with the amine groups of SeCA. The group tested the catalytic NO release capability of the graft, in which total NO from NO donors was released within 3 h. Other in vitro tests were conducted such as fibroblast proliferation and SMC spreading, which showed acceptable results when compared to the bare polycaprolactone graft.¹⁰⁸

Finally, they tested the samples in vivo using rats, in which the results (studied by scanning electron and normal microscopy) showed that selenium catalyst containing grafts had the least thrombus formation, compared with the control samples.

Similarly, in 2015, another study by Wang et al.¹⁰⁹ fabricated vascular grafts containing multiple layers of selenium catalyst added on the surface using LBL method. The design could be summarized as follows: polycaprolactone film (prepared by electrospinning) was covered by a synthesized selenium polyethyleneimine (SePEI) polymer that contains a positive charge, followed by a layer of hyaluronic acid with a negative charge, in which this type of sample was labeled as PCL-(S/H)₁₀. Other samples contained nine bilayers of SePEI/HA, then it was finalized by a bilayer of hyaluronic acid with Arg-Glu-Asp-Val (REDV) fibronectin peptide, which recognizes $\alpha 4\beta 1$ integrin specifically expressed on the ECs membrane thus inducing endothelial cell attachment on the surface. The grafts showed rapid endothelialization with increased ECs to SMCs ratio. In addition, the endothelial cells were organized in a uniform pattern on the surface.

Copper catalyst NO releasing surfaces. It is noteworthy to mention that nitrosothiols are not only catalyzed in the presence of selenium but also in the presence of copper (I) or copper (II) free ions or in ligand-complex form.¹¹⁰ Scheme 2 provides an insight on the mechanism of NO release.¹¹¹ Furthermore, it was revealed that at low dose of



Scheme 2. The mechanism of NO release: Cu⁺¹ (copper (I)), Cu⁺² (copper (II)), and RSNO (nitrosothiol).

Cu, efficient NO release could be achieved, thus reducing the chance of any Cu toxicity.^{112–114}

Based on the catalytic activity of Cu, Luo et al.¹¹⁰ incorporated Cu particles in a collagen–catechol or catechol–epigallocatechin gallate film composites coated on stainless steel. Primarily, they tested the NO release rate after incubation in a nitrosothiol containing media and found that the rates of collagen/catechol and collagen/epigallocatechin gallate were 0.77×10^{-10} mol/cm²/min and 0.28×10^{-10} mol/cm²/min, respectively, which was higher and lower than the agreed natural NO release rate by endothelial cells ($0.5\text{--}4 \times 10^{-10}$ mol/cm²/min).¹¹⁵ They also tested quantitatively the Cu content in both samples; it was found that the collagen–catechol films had a higher Cu content than its epigallocatechin counterpart, explaining the difference in NO release rate. Other in vitro tests were performed by the group including platelet adhesion, SMCs proliferation, and most importantly ECs proliferation. The results were promising, in which the platelet activation and adhesion along with SMCs proliferation was inhibited to a great extent by the films containing Cu due to NO release. On the other hand, the proliferation of ECs was promoted in the samples containing NO donors and Cu, whereas no difference in number of cells was noticed in the Cu-containing samples in the absence of NO donor in the media.

Miscellaneous. Ferritin, a protein, is well known for its intracellular iron storage role in vivo. This protein stores Fe³⁺ inside its shell and serves as an antioxidant protein, preventing excess iron from taking part in reactive oxygen species production by Fenton reaction.¹¹⁶ It is made up of a shell consisting of 24 protein subunits (apoferritin) and a core with Fe³⁺ ions.¹¹⁷ Ferritin is found everywhere in tissues and serum, along with ferritin-binding proteins on a large number of well-known cell lines.¹¹⁸ Cell proliferation and differentiation, angiogenesis, neoplastic transformation, immunosuppression, and iron delivery are metabolic processes that extracellular ferritin is involved in.¹¹⁹ Due to the presence of iron in various heme-containing enzymes, iron is crucial for cellular metabolism.

On the other hand, solid-supported lipid bilayers (SLBs) is a versatile, biocompatible, and fluid cell membrane mimicking platform that have high potential in fabricating many biomedical devices including sensors.⁹⁹

Taking these into consideration, Satriano et al.¹¹⁶ fabricated a series of positively charged SLBs on the surface of glass (Figure 4) and immobilized the negatively charged ferritin on the surface of the bilayer. The different increasing graded positive charge strength was achieved by mixing zwitterionic phospholipid, 1-palmitoyl-2-oleoyl-sn-glycero-3-phosphocholine (POPC), with the positively charged phospholipid 1-palmitoyl-2-oleoyl-sn-glycero-3-ethylphosphocholine (POEPC) with different ratios. The samples were named according to the ratio of POEPC to POPC, in which EPC100 contained only POEPC, EPC5 contained 5%

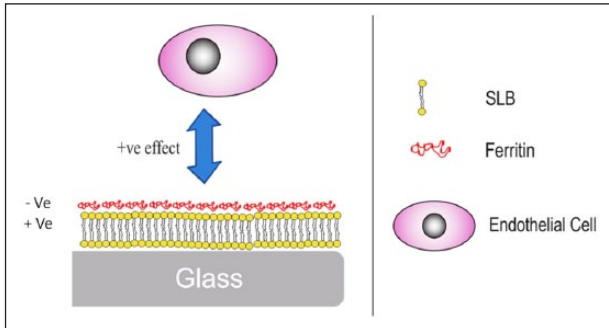


Figure 4. Schematic representation for the fabrication of ferritin-SLB system on the surface of glass.

POEPC and 95% POPC w/w. They tested the re-endothelializing ability of the different samples.

Initially, they tested the formation of the SLB and successful ferritin immobilization via quartz crystal microbalance with dissipation (QCM-D). The results showed that all the ratios formed a supported bilayer on the surface of silicon dioxide sensors with the formation taking two different formation kinetics depending on the charge strength of the vesicles.¹¹⁶ As the charge increased, the formation changed from two-step kinetics to one-step kinetics, which is in accordance with previously reported results.¹²⁰

The test results displayed that ferritin-coated SLB surfaces containing 25% POEPC had the largest amount of re-endothelialization among all the samples. With ferritin, the adhesion and proliferation of the ECs increased when compared to the controls.¹¹⁶

Substrate topography on re-endothelialization

Nanostructure formation. The surface morphology of material substrate could affect the migration of cells and the rate of endothelialization for successful stent implantation. Palmaz et al.¹²¹ studied the effects of surface topography of nitinol substrate, through introducing parallel grooves, on the growth of endothelial cells in an in vitro model. They found that grooved surfaces increased the migration rate of endothelial cells, particularly with larger grooves, when compared with control or smooth surfaces.¹²¹ Additional study has examined the effects of polystyrene and poly(4-bromostyrene) demixed islands with different nanoscale vertical dimensions (13, 35, and 95 nm) on the behavior of endothelial cells attachment and spreading.¹²² Based on islands depth, the cells showed different spreading interactions as nanometric topography which provide cues similar to those given by collagen. Interestingly, 13 nm islands presented the highest cell spreading morphologies with well-defined cytoskeleton.¹²² Choudhary et al.¹²³ investigated the adhesion of ECs and SMCs on random nanostructure compared with conventional titanium and cobalt-chromium substrates. They found that the adhesion and spreading morphologies of both cells were higher on

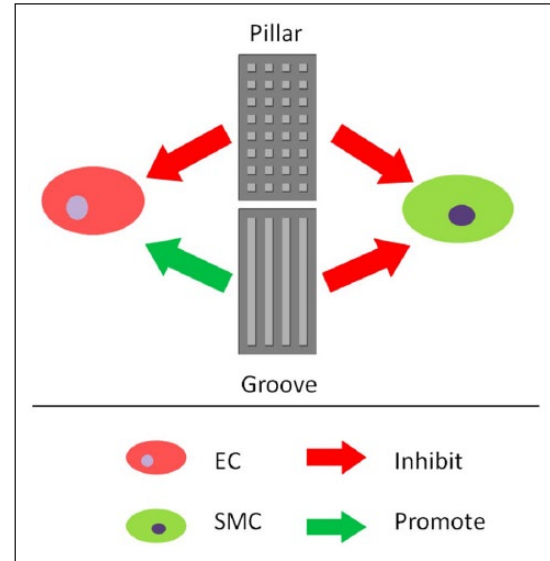


Figure 5. Schematic representation for the effect of surface morphology on proliferation of different types of cells.

the nanostructure substrate compared to the conventional substrate.¹²³ Moreover, the ratio of endothelial to SMCs was higher on nanostructure substrates.¹²³ However, it is well known that native endothelium adapts with aligned endothelial cell with elongated morphology; it can be expected that metallic stents with patterned surface may be better for increasing the functions of endothelial cell by promoting a more native cellular morphology. According to Lu et al., patterned nanostructure, with 750 nm, presented higher affinity toward rat aortic endothelial cells adhesion, growth, and alignment as compared with larger micrometer-scale titanium patterns as well as control with random nanostructures.¹²⁴ Recently, Ding et al.¹²⁵ fabricated micro/nano patterned platforms with two typical geometries (grove and pillar) with six sizes ranging between 0.5 and 50 μm and evaluated the cell and platelet responses (Figure 5). Based on the geometry, pillars presented nonselective SMCs inhibition and ECs growth. On the other hand, the size-dependent groove displayed selectivity through enhancing ECs growth and inhibiting SMCs proliferation.¹²⁵ Finally, they suggested that 1 μm patterned groove could perform as an optimum geometry for having various functionality of promoting re-endothelialization and inhibiting both of SMCs proliferation and platelet adhesion.¹²⁵

Nanotube formation. Several researchers have studied the effects of nanotube formation on cell behavior.^{126–128} Based on the nanotube size, the cells can interact with the surface selectively.¹²⁹ The nanotubes can reserve ECM nutrients which support cells and vessel physiology with health. In addition, nano-depot can store biomolecules or drugs and control release based on nanotube diameter and aspect ratio.^{130–132} The small bioactive molecules could be

released within weeks, whereas the big molecules could be released within several months.¹³¹ The diameter of hexagonally close-packed rigid nanopatterned adhesive dots interfaces ranged between 58 and 73 nm is required for cell attachment.^{133,134} The fabrication of TiO₂ nanotubes on titanium surface with average 100 nm outer diameter, 70 nm inner diameter, and 250 nm in height enhanced the migration of bovine aortic endothelial cells with faster speeds than on flat titanium surface.¹³⁴ It has been demonstrated that TiO₂ nanotubes represent a promising platform for stent as it could selectively regulate ECs growth and SMCs inhibition.^{135,136} Lee et al.¹³⁷ performed an upright nanotubular coating on nitinol substrate via anodization and investigated the effect of nanotubes on human aortic endothelial cells (HAEC) and human aortic smooth muscle cells (HASMC). Recently, in 2016, nitinol-based nanotubular coatings with 110 and 70 nm nanotube diameters, obtained by changing the anodization conditions, were used to investigate the effect of nanotube diameter on the functions of HAEC and HASMC.¹³⁸ They found that nanotubular coatings reduced HASMC proliferation and increased the migration, elastin, and collagen production of HAEC.¹³⁸ Interestingly, increased nanotube diameter improved the production of elastin and soluble collagen production, which could reduce the in-stent restenosis.¹³⁸ Another group reported the formation of two different kinds of TiO₂ nanotubes: (a) homogeneous nanotubes with average inner diameter of 75 nm and (b) heterogeneous nanotubes with average inner diameter of 80–190 nm.¹³⁰ They found that the endothelial cells have better proliferation rate on the homogeneous nanotubes when compared to heterogeneous nanotubes which could be due to better distribution of ions, proteins, and nutrients required for cells growth for homogeneous nanotubes.¹³⁰

Surface topography and chemistry for re-endothelialization

The surface topography as well as the surface chemistry have been shown to regulate the function and growth of cells. Recently, the combinations of both topography and chemistry of surfaces have attracted a great attention from researchers. Ding et al.¹³⁹ studied the impacts of immobilized heparin on topographically patterned substrates on the blood compatibility and re-endothelialization. According to their previous studies, 1 μm grooves on the TiO₂ substrates enhanced ECs growth, but inhibited SMCs proliferation and platelet adhesion.¹²⁵ The heparin-immobilized patterned TiO₂ substrates significantly promoted the growth of ECs and inhibited the proliferation of SMCs and platelet adhesion as compared to the corresponding heparin-immobilized flat surface.¹³⁹ The chemical effect of heparin was studied by grafting on two different topographic geometries, that is, groove versus pillar, with different topographic sizes ranging between 1 and 50 μm. It

was found that groove surface showed higher effect compared to pillars. In addition, the chemical effects increased with increasing the pattern size.¹³⁹ Although the main effect was for heparin chemistry, the surface topography was the reason to get aligned and elongated cells, which could achieve an accelerated healthy re-endothelialization and excellent blood compatibility.¹³⁹ Previous studies demonstrated that elongated and cytoskeletal aligned ECs on micropatterned surfaces decreased EC immunogenic gene expression and function which might contribute to EC-mediated atheroprotection.¹⁴⁰ Moreover, the nanopattern surface significantly enhanced the cell retention under shear flow.¹⁴¹

In 2014, Yang et al. developed a multifunctional surface with nanotubular TiO₂ structure modified with polydopamine in order to control the release of bivalirudin as direct thrombin inhibitor.¹⁴² The released bivalirudin was continued for 2 months with thrombin inhibitory bioactivity. Moreover, this surface presented high selectivity to enhance ECs growth and inhibit SMCs proliferation.¹⁴² Another strategy was reported in 2015 by Nie et al.,¹⁴³ which includes the modification of polyvinylidene difluoride (PVDF) membranes using a combination of carbon nanotube fibrous structure and heparin or heparin-like polymer. The nanofibrous heparin or heparin-like polymer multi-layers presented excellent antithrombotic activities and promoted endothelialization.¹⁴³

Summary

Due to the importance of re-endothelialization in preventing many diseases such as restenosis, in this review, copious endothelial cell-promoting strategies have been summarized, starting with surface chemistry modifications, passing through biomolecules(s) immobilization on surfaces and NO releasing surfaces, and ending with surface topography modification. At the end of this review, we believe that next-generation devices could combine both surface chemistry and topography in order to initiate specific cell responses and consequently accelerate re-endothelialization for vascular applications including stents.

Acknowledgements

T.M.B. and M.A.E. contributed equally to this work.

Declaration of conflicting interests

The author(s) declared no potential conflicts of interest with respect to the research, authorship, and/or publication of this article.

Funding

The author(s) disclosed receipt of the following financial support for the research, authorship, and/or publication of this article: This work was supported by Basic Science Research Program (2017R1A2B3011121), Cell Regeneration Program (2012M2A9

C6049717), Bio&Medical Technology Development Program (2014M3A9D3033887), and Korea Institute of Science and Technology (KIST) Program (2E26900) through the National Research Foundation funded by the Ministry of Science, ICT & Future Planning (MSIP) and 2017 International R&D Academy (IRDA) Alumni Partnership Project (2Z05100-17-089) funded by KIST, Seoul, Republic of Korea.

References

- Elnaggar MA, Joung YK and Han DK. Advanced stents for cardiovascular applications. In: Jo H, Jun HW, Shin J, et al. (eds) *Biomedical engineering: frontier research and converging technologies*. Cham: Springer International Publishing, 2016, pp. 407–426.
- Finegold JA, Asaria P and Francis DP. Mortality from ischaemic heart disease by country, region, and age: statistics from World Health Organization and United Nations. *Int J Cardiol* 2013; 168(2): 934–945.
- Serruys PW, de Jaegere P, Kiemeneij F, et al. A comparison of balloon-expandable-stent implantation with balloon angioplasty in patients with coronary artery disease. Benestent Study Group. *N Engl J Med* 1994; 331(8): 489–495.
- Holmes DR, Vlietstra RE, Smith HC, Jr, et al. Restenosis after percutaneous transluminal coronary angioplasty (PTCA): a report from the PTCA registry of the national heart, lung, and blood institute. *Am J Cardiol* 1984; 53(12): C77–C81.
- Fischman DL, Leon MB, Baim DS, et al. A randomized comparison of coronary-stent placement and balloon angioplasty in the treatment of coronary artery disease. *N Engl J Med* 1994; 331(8): 496–501.
- Kim SM, Park S-B, Bedair TM, et al. The effect of solvents and hydrophilic additive on stable coating and controllable sirolimus release system for drug-eluting stent. *Mater Sci Eng C Mater Biol Appl* 2017; 78: 39–46.
- Bedair TM, Kang SN, Joung YK, et al. A promising approach for improving the coating stability and in vivo performance of biodegradable polymer-coated sirolimus-eluting stent. *J Biomed Nanotechnol* 2016; 12(11): 2015–2028.
- Bedair TM, Yu SJ, Im SG, et al. Effects of interfacial layer wettability and thickness on the coating morphology and sirolimus release for drug-eluting stent. *J Colloid Interface Sci* 2015; 460: 189–199.
- Cho Y, Vu BQ, Bedair TM, et al. Crack prevention of biodegradable polymer coating on metal facilitated by a nanocoupled interlayer. *Journal of Bioactive and Compatible Polymers* 2014; 29(5): 515–526.
- Bedair TM, Cho Y, Joung YK, et al. Biodegradable polymer brush as nanocoupled interface for improving the durability of polymer coating on metal surface. *Colloids Surf B Biointerfaces* 2014; 122: 808–817.
- Bedair TM, Cho Y, Kim TJ, et al. Reinforcement of interfacial adhesion of a coated polymer layer on a cobalt-chromium surface for drug-eluting stents. *Langmuir* 2014; 30(27): 8020–8028.
- Sharif F, Hynes SO, McCullagh KJA, et al. Gene-eluting stents: non-viral, liposome-based gene delivery of eNOS to the blood vessel wall in vivo results in enhanced endothelialization but does not reduce restenosis in a hypercholesterolemic model. *Gene Ther* 2012; 19(3): 321–328.
- Carter AJ, Aggarwal M, Kopia GA, et al. Long-term effects of polymer-based, slow-release, sirolimus-eluting stents in a porcine coronary model. *Cardiovasc Res* 2004; 63(4): 617–624.
- Joner M, Finn AV, Farb A, et al. Pathology of drug-eluting stents in humans: delayed healing and late thrombotic risk. *J Am Coll Cardiol* 2006; 48(1): 193–202.
- Tan A, Farhatnia Y, de Mel A, et al. Inception to actualization: next generation coronary stent coatings incorporating nanotechnology. *J Biotechnol* 2013; 164(1): 151–170.
- Garg S and Serruys PW. Coronary stents: looking forward. *J Am Coll Cardiol* 2010; 56(Suppl. 10): S43–S78.
- Windecker S and Meier B. Late coronary stent thrombosis. *Circulation* 2007; 116(17): 1952–1965.
- Finn AV, Joner M, Nakazawa G, et al. Pathological correlates of late drug-eluting stent thrombosis: strut coverage as a marker of endothelialization. *Circulation* 2007; 115(18): 2435–2441.
- Pilgrim T and Windecker S. Drug-eluting stent thrombosis. *Minerva Cardioangiolog* 2009; 57(5): 611–620.
- Li G, Yang P, Qin W, et al. The effect of coimmobilizing heparin and fibronectin on titanium on hemocompatibility and endothelialization. *Biomaterials* 2011; 32(21): 4691–4703.
- Boyle JP, Smart RH and Shirey JK. Heparin in the treatment of chronic obstructive bronchopulmonary disease. *Am J Cardiol* 1964; 14(1): 25–28.
- Björk I and Lindahl U. Mechanism of the anticoagulant action of heparin. *Mol Cell Biochem* 1982; 48(3): 161–182.
- Linhardt RJ. 2003 Claude S. Hudson award address in carbohydrate chemistry. Heparin: structure and activity. *J Med Chem* 2003; 46(13): 2551–2564.
- Hoshi RA, Van Lith R, Jen MC, et al. The blood and vascular cell compatibility of heparin-modified ePTFE vascular grafts. *Biomaterials* 2013; 34(1): 30–41.
- Pan CJ, Pang LQ, Gao F, et al. Anticoagulation and endothelial cell behaviors of heparin-loaded graphene oxide coating on titanium surface. *Mater Sci Eng C Mater Biol Appl* 2016; 63: 333–340.
- Ahn YK, Jeong MH, Kim JW, et al. Preventive effects of the heparin-coated stent on restenosis in the porcine model. *Catheter Cardiovasc Interv* 1999; 48(3): 324–330.
- Boisson-Vidal C, Chaubet F, Chevolut L, et al. Relationship between antithrombotic activities of fucans and their structure. *Drug Develop Res* 2000; 51(4): 216–224.
- Matou S, Helley D, Chabut D, et al. Effect of fucoidan on fibroblast growth factor-2-induced angiogenesis in vitro. *Thromb Res* 2002; 106(4–5): 213–221.
- Park HY, Han MH, Park C, et al. Anti-inflammatory effects of fucoidan through inhibition of NF- κ B, MAPK and Akt activation in lipopolysaccharide-induced BV2 microglia cells. *Food Chem Toxicol* 2011; 49(8): 1745–1752.
- Li B, Lu F, Wei X, et al. Fucoidan: structure and bioactivity. *Molecules* 2008; 13(8): 1671–1695.

31. Cumashi A, Ushakova NA, Preobrazhenskaya ME, et al. A comparative study of the anti-inflammatory, anticoagulant, antiangiogenic, and antiadhesive activities of nine different fucoidans from brown seaweeds. *Glycobiology* 2007; 17(5): 541–552.
32. Deux JF, Meddahi-Pelle A, Bree F, et al. Comparative studies on the mechanisms of action of four polysaccharides on arterial restenosis. *J Biomater Sci Polym* 2009; 20(5–6): 689–702.
33. Deux JF, Meddahi-Pelle A, Le Blanche AF, et al. Low molecular weight fucoidan prevents neointimal hyperplasia in rabbit iliac artery in-stent restenosis model. *Arterioscler Thromb Vasc Biol* 2002; 22(10): 1604–1609.
34. Kim JM, Bae I-H, Lim KS, et al. A method for coating fucoidan onto bare metal stent and in vivo evaluation. *Prog Org Coat* 2015; 78: 348–356.
35. Roux N, Brakenhielm E, Freguin-Bouillant C, et al. Progenitor cell mobilizing treatments prevent experimental transplant arteriosclerosis. *J Surg Res* 2012; 176(2): 657–665.
36. Bouvard C, Galy-Fauroux I, Grelac F, et al. Low-molecular-weight fucoidan induces endothelial cell migration via the PI3K/AKT pathway and modulates the transcription of genes involved in angiogenesis. *Mar Drugs* 2015; 13(12): 7446–7462.
37. Raymond M-A, Desormeaux A, Laplante P, et al. Apoptosis of endothelial cells triggers a caspase-dependent anti-apoptotic paracrine loop active on vascular smooth muscle cells. *FASEB J* 2004; 18(6): 705–707.
38. Keuren JFW, Wielders SJH, Willems GM, et al. Thrombogenicity of polysaccharide-coated surfaces. *Biomaterials* 2003; 24(11): 1917–1924.
39. Tian WM, Zhang CL, Hou SP, et al. Hyaluronic acid hydrogel as Nogo-66 receptor antibody delivery system for the repairing of injured rat brain: in vitro. *J Control Release* 2005; 102(1): 13–22.
40. Markwald RR, Fitzharris TP and Bernanke DH. Morphologic recognition of complex carbohydrates in embryonic cardiac extracellular matrix. *J Histochem Cytochem* 1979; 27(8): 1171–1173.
41. Schanté CE, Zuber G, Herlin C, et al. Chemical modifications of hyaluronic acid for the synthesis of derivatives for a broad range of biomedical applications. *Carbohydr Polym* 2011; 85(3): 469–489.
42. You H, Lee E-U, Kim Y-K, et al. Biocompatibility and resorption pattern of newly developed hyaluronic acid hydrogel reinforced three-layer poly (lactide-co-glycolide) membrane: histologic observation in rabbit calvarial defect model. *Biomater Res* 2014; 18: 12.
43. Verheye S, Markou CP, Salame MY, et al. Reduced thrombus formation by hyaluronic acid coating of endovascular devices. *Arterioscler Thromb Vasc Biol* 2000; 20(4): 1168–1172.
44. Masson JF, Battaglia TM, Davidson MJ, et al. Biocompatible polymers for antibody support on gold surfaces. *Talanta* 2005; 67(5): 918–925.
45. Liu X, Huang R, Su R, et al. Grafting hyaluronic acid onto gold surface to achieve low protein fouling in surface plasmon resonance biosensors. *ACS Appl Mater Interfaces* 2014; 6(15): 13034–13042.
46. Bauer S, Arpa-Sancet MP, Finlay JA, et al. Adhesion of marine fouling organisms on hydrophilic and amphiphilic polysaccharides. *Langmuir* 2013; 29(12): 4039–4047.
47. Ramadan MH, Prata JE, Karacsony O, et al. Reducing protein adsorption with polymer-grafted hyaluronic acid coatings. *Langmuir* 2014; 30(25): 7485–7495.
48. Ho CT, Chen Q, Shi H, et al. Antioxidative effect of polyphenol extract prepared from various Chinese teas. *Prev Med* 1992; 21(4): 520–525.
49. Abu-Amsha Caccetta R, Burke V, Mori TA, et al. Red wine polyphenols, in the absence of alcohol, reduce lipid peroxidative stress in smoking subjects. *Free Radic Biol Med* 2001; 30(6): 636–642.
50. Stangl V, Dreger H, Stangl K, et al. Molecular targets of tea polyphenols in the cardiovascular system. *Cardiovasc Res* 2007; 73(2): 348–358.
51. Inoue M, Suzuki R, Sakaguchi N, et al. Selective induction of cell death in cancer cells by gallic acid. *Biol Pharm Bull* 1995; 18(11): 1526–1530.
52. Kang MS, Oh JS, Kang IC, et al. Inhibitory effect of methyl gallate and gallic acid on oral bacteria. *J Microbiol* 2008; 46(6): 744–750.
53. Kratz JM, Andrighetti-Frohner CR, Leal PC, et al. Evaluation of anti-HSV-2 activity of gallic acid and pentyl gallate. *Biol Pharm Bull* 2008; 31(5): 903–907.
54. Kim SH, Jun CD, Suk K, et al. Gallic acid inhibits histamine release and pro-inflammatory cytokine production in mast cells. *Toxicol Sci* 2006; 91(1): 123–131.
55. Chen HM, Wu YC, Chia YC, et al. Gallic acid, a major component of *Toona sinensis* leaf extracts, contains a ROS-mediated anti-cancer activity in human prostate cancer cells. *Cancer Lett* 2009; 286(2): 161–171.
56. Inoue M, Sakaguchi N, Isuzugawa K, et al. Role of reactive oxygen species in gallic acid-induced apoptosis. *Biol Pharm Bull* 2000; 23(10): 1153–1157.
57. Qiu X, Takemura G, Koshiji M, et al. Gallic acid induces vascular smooth muscle cell death via hydroxyl radical production. *Heart Vessels* 2000; 15(2): 90–99.
58. He Y, Wang J, Yan W, et al. Gallic acid and gallic acid-loaded coating involved in selective regulation of platelet, endothelial and smooth muscle cell fate. *RSC Adv* 2014; 4(1): 212–221.
59. Von der Mark K and Park J. Engineering biocompatible implant surfaces: part II: cellular recognition of biomaterial surfaces: lessons from cell–matrix interactions. *Prog Mater Sci* 2013; 58(3): 327–381.
60. Wang C-H, Wang T-M, Young T-H, et al. The critical role of ECM proteins within the human MSC niche in endothelial differentiation. *Biomaterials* 2013; 34(17): 4223–4234.
61. Barbucci R, Magnani A, Chiumiento A, et al. Fibroblast cell behavior on bound and adsorbed fibronectin onto hyaluronan and sulfated hyaluronan substrates. *Biomacromolecules* 2005; 6(2): 638–645.
62. Lee MH, Ducheyne P, Lynch L, et al. Effect of biomaterial surface properties on fibronectin- $\alpha 5\beta 1$ integrin interaction and cellular attachment. *Biomaterials* 2006; 27(9): 1907–1916.
63. Davis DH, Giannoulis CS, Johnson RW, et al. Immobilization of RGD to $\langle 111 \rangle$ silicon surfaces for enhanced cell adhesion and proliferation. *Biomaterials* 2002; 23(19): 4019–4027.

64. Yin Y, Wise SG, Nosworthy NJ, et al. Covalent immobilization of tropoelastin on a plasma deposited interface for enhancement of endothelialisation on metal surfaces. *Biomaterials* 2009; 30(9): 1675–1681.
65. Meldal M and Schoffelen S. Recent advances in covalent, site-specific protein immobilization. *F1000Res* 2016; 5: 1–11.
66. Jung Y, Jeong JY and Chung BH. Recent advances in immobilization methods of antibodies on solid supports. *Analyst* 2008; 133(6): 697–701.
67. Yang Y, Qi P, Wen F, et al. Mussel-inspired one-step adherent coating rich in amine groups for covalent immobilization of heparin: hemocompatibility, growth behaviors of vascular cells, and tissue response. *ACS Appl Mater Interfaces* 2014; 6(16): 14608–14620.
68. Ma L, Qin H, Cheng C, et al. Mussel-inspired self-coating at macro-interface with improved biocompatibility and bioactivity via dopamine grafted heparin-like polymers and heparin. *J Mater Chem B* 2014; 2(4): 363–375.
69. Li M, Wu H, Wang Y, et al. Immobilization of heparin/poly-L-lysine microspheres on medical grade high nitrogen nickel-free austenitic stainless steel surface to improve the biocompatibility and suppress thrombosis. *Mater Sci Eng C Mater Biol Appl* 2017; 73: 198–205.
70. Thalla PK, Fadlallah H, Liberelle B, et al. Chondroitin sulfate coatings display low platelet but high endothelial cell adhesive properties favorable for vascular implants. *Biomacromolecules* 2014; 15(7): 2512–2520.
71. Kim SM, Park KS, Lih E, et al. Fabrication and characteristics of dual functionalized vascular stent by spatio-temporal coating. *Acta Biomater* 2016; 38: 143–152.
72. Lih E, Choi SG, Ahn DJ, et al. Optimal conjugation of catechol group onto hyaluronic acid in coronary stent substrate coating for the prevention of restenosis. *J Tissue Eng* 2016; 7: 2041731416683745.
73. Huang R, Liu X, Ye H, et al. Conjugation of hyaluronic acid onto surfaces via the interfacial polymerization of dopamine to prevent protein adsorption. *Langmuir* 2015; 31(44): 12061–12070.
74. Yang Z, Xiong K, Qi P, et al. Gallic acid tailoring surface functionalities of plasma-polymerized allylamine-coated 316L SS to selectively direct vascular endothelial and smooth muscle cell fate for enhanced endothelialization. *ACS Appl Mater Interfaces* 2014; 6(4): 2647–2656.
75. Cheng XW, Kuzuya M, Nakamura K, et al. Mechanisms of the inhibitory effect of epigallocatechin-3-gallate on cultured human vascular smooth muscle cell invasion. *Arterioscler Thromb Vasc Biol* 2005; 25(9): 1864–1870.
76. Isemura M, Saeki K, Kimura T, et al. Tea catechins and related polyphenols as anti-cancer agents. *Biofactors* 2000; 13(1–4): 81–85.
77. Kim SY, Jin YR, Lim Y, et al. Inhibition of PDGF beta-receptor tyrosine phosphorylation and its downstream intracellular signal transduction in rat aortic vascular smooth muscle cells by kaempferol. *Planta Med* 2005; 71(7): 599–603.
78. Kim DW, Park YS, Kim YG, et al. Local delivery of green tea catechins inhibits neointimal formation in the rat carotid artery injury model. *Heart Vessels* 2004; 19(5): 242–247.
79. Lu LH, Lee SS and Huang HC. Epigallocatechin suppression of proliferation of vascular smooth muscle cells: correlation with c-jun and JNK. *Br J Pharmacol* 1998; 124(6): 1227–1237.
80. Chyu KY, Babbidge SM, Zhao X, et al. Differential effects of green tea-derived catechin on developing versus established atherosclerosis in apolipoprotein E-null mice. *Circulation* 2004; 109(20): 2448–2453.
81. He T, Yang Z, Chen R, et al. Enhanced endothelialization guided by fibronectin functionalized plasma polymerized acrylic acid film. *Mater Sci Eng C Mater Biol Appl* 2012; 32(5): 1025–1031.
82. Wang X, Liu T, Chen Y, et al. Extracellular matrix inspired surface functionalization with heparin, fibronectin and VEGF provides an anticoagulant and endothelialization supporting microenvironment. *Appl Surf Sci* 2014; 320: 871–882.
83. Han F, Jia X, Dai D, et al. Performance of a multilayered small-diameter vascular scaffold dual-loaded with VEGF and PDGF. *Biomaterials* 2013; 34(30): 7302–7313.
84. Shin YM, Lee YB, Kim SJ, et al. Mussel-inspired immobilization of Vascular Endothelial Growth Factor (VEGF) for enhanced endothelialization of vascular grafts. *Biomacromolecules* 2012; 13(7): 2020–2028.
85. Anderson SM, Siegman SN and Segura T. The effect of Vascular Endothelial Growth Factor (VEGF) presentation within fibrin matrices on endothelial cell branching. *Biomaterials* 2011; 32(30): 7432–7443.
86. Choi DH, Kang SN, Kim SM, et al. Growth factors-loaded stents modified with hyaluronic acid and heparin for induction of rapid and tight re-endothelialization. *Colloid Surf B* 2016; 141: 602–610.
87. Ye C, Wang Y, Su H, et al. Construction of a fucoidan/laminin functional multilayer to direction vascular cell fate and promotion hemocompatibility. *Mater Sci Eng C Mater Biol Appl* 2016; 64: 236–242.
88. Tang ZY, Wang Y, Podsiadlo P, et al. Biomedical applications of layer-by-layer assembly: from biomimetics to tissue engineering. *Adv Mater* 2006; 18(24): 3203–3224.
89. Decher G, Hong JD and Schmitt J. Buildup of ultrathin multilayer films by a self-assembly process: III. Consecutively alternating adsorption of anionic and cationic polyelectrolytes on charged surfaces. *Thin Solid Films* 1992; 210: 831–835.
90. Wang Y, Ye C, Su H, et al. Layer-by-layer self-assembled laminin/fucoidan films: towards better hemocompatibility and endothelialization. *RSC Adv* 2016; 6(61): 56048–56055.
91. Wang HG, Yin TY, Ge SP, et al. Biofunctionalization of titanium surface with multilayer films modified by heparin-VEGF-fibronectin complex to improve endothelial cell proliferation and blood compatibility. *J Biomed Mater Res A* 2013; 101(2): 413–420.
92. Liu P, Zhao Y, Yan Y, et al. Construction of extracellular microenvironment to improve surface endothelialization of NiTi alloy substrate. *Mater Sci Eng C Mater Biol Appl* 2015; 55: 1–7.
93. Elnaggar MA, Seo SH, Gobaa S, et al. Nitric oxide releasing coronary stent: a new approach using layer-by-layer coating and liposomal encapsulation. *Small* 2016; 12(43): 6012–6023.

94. Tanner FC, Meier P, Greutert H, et al. Nitric oxide modulates expression of cell cycle regulatory proteins: a cytostatic strategy for inhibition of human vascular smooth muscle cell proliferation. *Circulation* 2000; 101(16): 1982–1989.
95. Kapadia MR, Eng JW, Jiang Q, et al. Nitric oxide regulates the 26S proteasome in vascular smooth muscle cells. *Nitric Oxide* 2009; 20(4): 279–288.
96. Gooch KJ, Dangler CA and Frangos JA. Exogenous, basal, and flow-induced nitric oxide production and endothelial cell proliferation. *J Cell Physiol* 1997; 171(3): 252–258.
97. Ishida A, Sasaguri T, Kosaka C, et al. Induction of the cyclin-dependent kinase inhibitor p21(Sdi1/Cip1/Waf1) by nitric oxide-generating vasodilator in vascular smooth muscle cells. *J Biol Chem* 1997; 272(15): 10050–10057.
98. Taylor EL, Li JT, Tupper JC, et al. GEA 3162, a peroxynitrite donor, induces Bcl-2-sensitive, p53-independent apoptosis in murine bone marrow cells. *Biochem Pharmacol* 2007; 74(7): 1039–1049.
99. Elnaggar MA, Subbiah R, Han DK, et al. Lipid-based carriers for controlled delivery of nitric oxide. *Expert Opin Drug Deliv*. Epub ahead of print 6 February 2017. DOI: 10.1080/17425247.2017.1285904.
100. Kelm M. Nitric oxide metabolism and breakdown. *Biochim Biophys Acta* 1999; 1411(2–3): 273–289.
101. Mathews SM, Spallholz JE, Grimson MJ, et al. Prevention of bacterial colonization of contact lenses with covalently attached selenium and effects on the rabbit cornea. *Cornea* 2006; 25(7): 806–814.
102. Hou Y, Guo Z, Li J, et al. Seleno compounds and glutathione peroxidase catalyzed decomposition of S-Nitrosothiols. *Biochem Biophys Res Commun* 1996; 228(1): 88–93.
103. Cha W and Meyerhoff ME. Catalytic generation of nitric oxide from S-nitrosothiols using immobilized organoselenium species. *Biomaterials* 2007; 28(1): 19–27.
104. Freedman JE, Frei B, Welch GN, et al. Glutathione peroxidase potentiates the inhibition of platelet function by S-nitrosothiols. *J Clin Invest* 96(1): 394–400.
105. Weng Y, Song Q, Zhou Y, et al. Immobilization of selenocystamine on TiO₂ surfaces for in situ catalytic generation of nitric oxide and potential application in intravascular stents. *Biomaterials* 2011; 32(5): 1253–1263.
106. Yang Z, Yang Y, Xiong K, et al. Nitric oxide producing coating mimicking endothelium function for multifunctional vascular stents. *Biomaterials* 2015; 63: 80–92.
107. Yang Z, Lei X, Wang J, et al. A novel technique toward bipolar films containing alternating nano-layers of allylamine and acrylic acid plasma polymers for biomedical application. *Plasma Process Polym* 2011; 8(3): 208–214.
108. Chen S, An J, Weng L, et al. Construction and biofunctional evaluation of electrospun vascular graft loaded with selenocystamine for in situ catalytic generation of nitric oxide. *Mater Sci Eng C Mater Biol Appl* 2014; 45: 491–496.
109. Wang Y, Chen S, Pan Y, et al. Rapid in situ endothelialization of a small diameter vascular graft with catalytic nitric oxide generation and promoted endothelial cell adhesion. *J Mat Chem B* 2015; 3(47): 9212–9222.
110. Luo R, Liu Y, Yao H, et al. Copper-incorporated collagen/catechol film for in situ generation of nitric oxide. *ACS Biomater Sci Eng* 2015; 1(9): 771–779.
111. Noble DR, Swift HR and Williams DLH. Nitric oxide release from S-nitrosoglutathione (GSNO). *Chem Commun* 1999; 22: 2317–2318.
112. Williams DLH. The mechanism of nitric oxide formation from S-nitrosothiols (thionitrites). *Chem Commun* 1996; 10: 1085–1091.
113. Gorren ACF, Schrammel A, Schmidt K, et al. Decomposition of S-Nitrosoglutathione in the presence of copper ions and glutathione. *Arch Biochem Biophys* 1996; 330(2): 219–228.
114. Herves Beloso P and Williams DLH. Reversibility of S-nitrosothiol formation. *Chem Commun* 1997; 1: 89–90.
115. Vaughn MW, Kuo L and Liao JC. Estimation of nitric oxide production and reaction rates in tissue by use of a mathematical model. *Am J Physiol* 1998; 274(6): H2163–H2176.
116. Satriano C, Lupo G, Motta C, et al. Ferritin-supported lipid bilayers for triggering the endothelial cell response. *Colloid Surf B* 2017; 149: 48–55.
117. Arosio P, Adelman TG and Drysdale JW. On ferritin heterogeneity. Further evidence for heteropolymers. *J Biol Chem* 1978; 253(12): 4451–4458.
118. Moss D, Powell LW, Halliday JW, et al. Functional roles of the ferritin receptors of human liver, hepatoma, lymphoid and erythroid cells. *J Inorg Biochem* 47(1): 219–227.
119. Torti SV and Torti FM. Iron and cancer: more ore to be mined. *Nat Rev Cancer* 2013; 13(5): 342–355.
120. Richter R, Mukhopadhyay A and Brisson A. Pathways of lipid vesicle deposition on solid surfaces: a combined QCM-D and AFM study. *Biophys J* 2003; 85(5): 3035–3047.
121. Palmaz JC, Benson A and Sprague EA. Influence of surface topography on endothelialization of intravascular metallic material. *J Vasc Interv Radiol* 1999; 10(4): 439–444.
122. Dalby MJ, Riehle MO, Johnstone H, et al. In vitro reaction of endothelial cells to polymer demixed nanotopography. *Biomaterials* 2002; 23(14): 2945–2954.
123. Choudhary S, Berhe M, Haberstroh KM, et al. Increased endothelial and vascular smooth muscle cell adhesion on nanostructured titanium and CoCrMo. *Int J Nanomed* 2006; 1(1): 41–49.
124. Lu J, Rao MP, MacDonald NC, et al. Improved endothelial cell adhesion and proliferation on patterned titanium surfaces with rationally designed, micrometer to nanometer features. *Acta Biomater* 2008; 4(1): 192–201.
125. Ding Y, Yang Z, Bi CWC, et al. Directing vascular cell selectivity and hemocompatibility on patterned platforms featuring variable topographic geometry and size. *ACS Appl Mater Interfaces* 2014; 6(15): 12062–12070.
126. Oh S, Daraio C, Chen L-H, et al. Significantly accelerated osteoblast cell growth on aligned TiO₂ nanotubes. *J Biomed Mater Res A* 2006; 78(1): 97–103.
127. Park J, Bauer S, Von Mark K, et al. Nanosize and vitality: TiO₂ nanotube diameter directs cell fate. *Nano Lett* 2007; 7(6): 1686–1691.

128. Zhu X, Chen J, Scheideler L, et al. Cellular reactions of osteoblasts to micron- and submicron-scale porous structures of titanium surfaces. *Cells Tissues Organs* 2004; 178(1): 13–22.
129. Brammer KS, Oh S, Cobb CJ, et al. Improved bone-forming functionality on diameter-controlled TiO₂ nanotube surface. *Acta Biomater* 2009; 5(8): 3215–3223.
130. Saleh YE, Gepreel MA and Allam NK. Functional nano-architectures for enhanced drug eluting stents. *Sci Rep* 2017; 7: 40291.
131. Peng L, Mendelsohn AD, LaTempa TJ, et al. Long-term small molecule and protein elution from TiO₂ nanotubes. *Nano Lett* 2009; 9(5): 1932–1936.
132. Song Y-Y, Schmidt-Stein F, Bauer S, et al. Amphiphilic TiO₂ nanotube arrays: an actively controllable drug delivery system. *J Am Chem Soc* 2009; 131(12): 4230–4232.
133. Arnold M, Cavalcanti-Adam EA, Glass R, et al. Activation of integrin function by nanopatterned adhesive interfaces. *Chem Phys Chem* 2004; 5(3): 383–388.
134. Brammer KS, Oh S, Gallagher JO, et al. Enhanced cellular mobility guided by TiO₂ nanotube surfaces. *Nano Lett* 2008; 8(3): 786–793.
135. Peng L, Eltgroth ML, LaTempa TJ, et al. The effect of TiO₂ nanotubes on endothelial function and smooth muscle proliferation. *Biomaterials* 2009; 30(7): 1268–1272.
136. Peng L, Barczak AJ, Barbeau RA, et al. Whole genome expression analysis reveals differential effects of TiO₂ nanotubes on vascular cells. *Nano Lett* 2010; 10(1): 143–148.
137. Lee PP, Cerchiari A and Desai TA. Nitinol-based nanotubular coatings for the modulation of human vascular cell function. *Nano Lett* 2014; 14(9): 5021–5028.
138. Lee PP and Desai TA. Nitinol-based nanotubular arrays with controlled diameters upregulate human vascular cell ECM production. *ACS Biomater Sci Eng* 2016; 2(3): 409–414.
139. Ding Y, Yang M, Yang Z, et al. Cooperative control of blood compatibility and re-endothelialization by immobilized heparin and substrate topography. *Acta Biomater* 2015; 15: 150–163.
140. Vartanian KB, Berny MA, McCarty OJT, et al. Cytoskeletal structure regulates endothelial cell immunogenicity independent of fluid shear stress. *Am J Physiol Cell Physiol* 2010; 298(2): C333.
141. Zorlutuna P, Rong Z, Vadgama P, et al. Influence of nanopatterns on endothelial cell adhesion: enhanced cell retention under shear stress. *Acta Biomater* 2009; 5(7): 2451–2459.
142. Yang Z, Zhong S, Yang Y, et al. Polydopamine-mediated long-term elution of the direct thrombin inhibitor bivalirudin from TiO₂ nanotubes for improved vascular biocompatibility. *J Mater Chem B* 2014; 2(39): 6767–6778.
143. Nie C, Ma L, Cheng C, et al. Nanofibrous heparin and heparin-mimicking multilayers as highly effective endothelialization and antithrombogenic coatings. *Biomacromolecules* 2015; 16(3): 992–1001.